

Lensing effect on polarization in microwave background: extracting convergence power spectrum

Jacek Guzik[†]

Astronomical Observatory, Jagiellonian University, Orla 171, 30-244 Kraków, Poland

Uroš Seljak[‡]

Department of Physics, Jadwin Hall, Princeton University, Princeton, NJ 08544

Matias Zaldarriaga^{††}

Institute for Advanced Studies, School of Natural Sciences, Princeton, NJ 08540

(October 1999)

Matter inhomogeneities along the line of sight deflect the cosmic microwave background (CMB) photons originating at the last scattering surface at redshift $z \sim 1100$. These distortions modify the pattern of CMB polarization. We identify specific combinations of Stokes Q and U parameters that correspond to spin $0, \pm 2$ variables and can be used to reconstruct the projected matter density. We compute the expected signal to noise as a function of detector sensitivity and angular resolution. With Planck satellite the detection would be at a few σ level. Several times better detector sensitivity would be needed to measure the projected dark matter power spectrum over a wider range of scales, which could provide an independent confirmation of the projected matter power spectrum as measured from other methods.

PACS numbers: 98.80.Es, 95.85.Bh, 98.35.Ce, 98.70.Vc

I. INTRODUCTION

Cosmic microwave background (CMB) is believed to originate from the epoch when protons and electrons recombined into neutral hydrogen making the universe transparent, which happened around redshift $z \sim 1100$. Photons travelling along the line of sight towards the observer were deflected by intervening dark matter distribution via the gravitational lensing effect. This process conserves two quantities: surface brightness and polarization. Conservation of surface brightness implies that in the absence of any fluctuations none can be generated by gravitational lensing. However, if there are fluctuations present then gravitational lensing can either smooth these out on large scales [1] or generate new fluctuations on small scales [3]. The effect of these distortions on the CMB anisotropies has been thoroughly investigated, both on the CMB power spectrum [1,2] as well as on the induced nongaussian signatures [4]. These studies have shown that the lensing effect is small, but detectable with future CMB experiments, and would provide important information on the distribution of dark matter up to $z \sim 1100$. This method possibly measures clustering amplitude at higher redshifts and larger scales than any other method and would be specially valuable in breaking the degeneracies between cosmological parameters present when one only uses the CMB data.

Given the potential importance of measuring the dark matter power spectrum on large scales and/or high redshifts, it is worth investigating other methods than can provide similar information. This is particularly important because any such measurement will only be statistical in nature and could be susceptible to various systematic effects. One such method is gravitational lensing on the CMB polarization. Polarization is also conserved by gravitational lensing so that the latter only moves the polarization tensor from one point to another conserving its amplitude and direction in the mapping. Since it is widely expected that CMB polarization will be detected with the future CMB experiments it is worth asking what kind of information can be learned from investigating the lensing effect on polarization and how can it be extracted.

The effect of lensing on the power spectrum of CMB polarization has already been explored in [5]. It has been shown there that lensing smoothes the acoustic peaks of E polarization and also generates a B -type polarization. While this induced B polarization is small, it provides a fundamental limit to the level of B polarization from other sources that can be detected on large scales. For example, it limits the detectable tensor to scalar ratios to be above 10^{-4} , although this is not a significant limitation for the near future.

In this paper we explore in more detail the prospects of directly detecting gravitational lensing effect on the CMB polarization through its nongaussian signatures. We show that there is a combination of derivatives of polarization that provide a local estimator of shear and convergence. These, while noisy, can be used to provide an estimator of

projected dark matter power spectrum, which by averaging over all the sky may yield a detectable signal. We compute the expected signal to noise as a function of detector sensitivity and apply it to the future satellite experiments.

II. CONVERGENCE FROM THE CMB POLARIZATION

In this section we develop a method to extract the gravitational lensing effect on polarization in the ideal case without detector noise and beam smoothing. Next section will deal with these complications. A radiation field can be fully described in terms of four Stokes parameters [6] or the specific intensity tensor I_{ij} . For the CMB the Stokes parameters can be chosen as the temperature anisotropy T proportional to the sum of intensities along two perpendicular directions in the sky¹, the Stokes parameter Q , defined as the difference between the intensities along the two axis and the Stokes parameter U , defined by the difference between intensities along the two diagonals. The fourth Stokes parameter V describes circular polarization which is not generated via the Thomson scattering believed to be the only generating mechanism for polarization, so we will ignore it in the following.

The Stokes parameters Q and U are two fields in the sky, which we assume to be Gaussian random fields that are generated from a common scalar potential (we ignore any initial B -type polarization, which, even if present, would likely be important only on large scales). Because gravitational lensing conserves polarization their observed values in the θ direction $Q(\theta)$ and $U(\theta)$ are related to their values at the recombination \tilde{Q} , \tilde{U} , deflected by an angle $\delta\theta$

$$\begin{aligned} Q(\theta) &= \tilde{Q}(\theta + \delta\theta) \\ U(\theta) &= \tilde{U}(\theta + \delta\theta). \end{aligned} \quad (1)$$

To extract the lensing information contained in these fields we consider their spatial derivatives. These can be written in the weak lensing regime as

$$\begin{aligned} Q_a(\theta) &= (\delta_{ab} + \Phi_{ab})\tilde{Q}_b(\theta + \delta\theta) \\ U_a(\theta) &= (\delta_{ab} + \Phi_{ab})\tilde{U}_b(\theta + \delta\theta), \end{aligned} \quad (2)$$

where $\Phi_{ab} = \frac{\partial\delta\theta_a}{\partial\theta_b}$ with $a, b = x, y$ are the shear tensor components describing the lensing effect.

Just like in the temperature case [7] we form quadratic combinations of derivatives of the Stokes parameters and express them in terms of unlensed variables and the components of the shear tensor. We wish to begin with a quantity that does not depend on the coordinate frame, which allows us to simply relate the unlensed and the lensed quantities. Such a quadratic quantity is readily available and is given by $Q^2 + U^2$. Then, in the lowest order, we have

$$\begin{aligned} \mathcal{S}_P &\equiv [Q_x^2 + Q_y^2 + U_x^2 + U_y^2](\theta) \\ &= (1 + \Phi_{xx} + \Phi_{yy})\tilde{\mathcal{S}}_P + (\Phi_{xx} - \Phi_{yy})\tilde{\mathcal{Q}}_P + 2\Phi_{xy}\tilde{\mathcal{U}}_P \\ \mathcal{Q}_P &\equiv [Q_x^2 - Q_y^2 + U_x^2 - U_y^2](\theta) \\ &= (1 + \Phi_{xx} + \Phi_{yy})\tilde{\mathcal{Q}}_P + (\Phi_{xx} - \Phi_{yy})\tilde{\mathcal{S}}_P \\ \mathcal{U}_P &\equiv [2Q_xQ_y + 2U_xU_y](\theta) \\ &= (1 + \Phi_{xx} + \Phi_{yy})\tilde{\mathcal{U}}_P + 2\Phi_{xy}\tilde{\mathcal{S}}_P, \end{aligned} \quad (3)$$

where subscripts x and y stand for respective derivatives in the real space. Equation (3) shows that the measured \mathcal{S}_P , \mathcal{Q}_P and \mathcal{U}_P are products of the shear tensor and derivatives of the unlensed CMB polarization field. Thus the power spectrum of \mathcal{S}_P , \mathcal{Q}_P and \mathcal{U}_P will be a convolution of the power in the CMB and that of the projected mass density. Convergence and unlensed fields are taken as independent quantities, which is a good approximation since most of the lensing power arises from low redshifts, which are not correlated with the last scattering surface. The general expression for this convolution is quite involved. Here we will discuss it in the limit of large scales relative to the CMB correlation length $\xi \sim 0.1^\circ$ where it is not necessary to take the full convolution into account. In the large scale limit patches of the sky larger than the correlation length squared are almost independent, which simplifies the

¹ We work in the small scale limit which simplifies the expressions. Since the final results indicate that lensing on polarization is not detectable on very large scales this does not impose a significant limitation on the present work.

calculations. This large scale limit is sufficient to analyze future data from MAP and Planck satellites and will, in any case, provide a lower limit to the attainable signal.

The reason we have chosen \mathcal{S}_P , \mathcal{Q}_P and \mathcal{U}_P as variables in consideration is that they have transformation properties similar to the Stokes parameters [6]. We wish to show that \mathcal{S}_P , \mathcal{Q}_P and \mathcal{U}_P transform as Stokes parameters during the right-handed rotation of the spatial base $(\hat{x}, \hat{y}, \hat{n})$ by an angle ψ around \hat{n} directed to the observer. Transformation of Stokes parameters Q and U under rotation are given in [8] and their linear combinations $Q \pm iU$ have values of spin equal to ∓ 2 ,

$$Q' \pm iU' = e^{\mp i2\psi} (Q \pm iU). \quad (4)$$

We can rewrite definitions of polarization variables (equation 3) in the following manner

$$\begin{aligned} \mathcal{S}_P &= (Q + iU)_x(Q - iU)_x + (Q + iU)_y(Q - iU)_y \\ \mathcal{Q}_P &= (Q + iU)_x(Q - iU)_x - (Q + iU)_y(Q - iU)_y \\ \mathcal{U}_P &= (Q + iU)_x(Q - iU)_y + (Q + iU)_y(Q - iU)_x. \end{aligned} \quad (5)$$

When we use equations (4) and (5) and change variables in derivatives we find the final expression for transformation of our quantities,

$$\begin{pmatrix} \mathcal{S}'_P \\ \mathcal{Q}'_P \\ \mathcal{U}'_P \end{pmatrix} = \begin{pmatrix} 1 & 0 & 0 \\ 0 & \cos 2\psi & \sin 2\psi \\ 0 & -\sin 2\psi & \cos 2\psi \end{pmatrix} \begin{pmatrix} \mathcal{S}_P \\ \mathcal{Q}_P \\ \mathcal{U}_P \end{pmatrix}.$$

This demonstrates that \mathcal{S}_P transforms as a scalar, while \mathcal{Q}_P and \mathcal{U}_P transform like respective Stokes parameters Q and U . We will show that these correspond to the familiar convergence and shear quantities of gravitational lensing.

In the large scale limit (compared to the correlation length of the CMB polarization field) and in the absence of lensing we can write the average over the ensemble of the CMB realizations

$$\begin{aligned} \langle \tilde{\mathcal{S}}_P \rangle_{CMB} &= \sigma_{SP} \\ \langle \tilde{\mathcal{Q}}_P \rangle_{CMB} &= 0 \\ \langle \tilde{\mathcal{U}}_P \rangle_{CMB} &= 0, \end{aligned} \quad (6)$$

where σ_{SP} is defined as

$$\sigma_{SP} = \langle Q_x^2 \rangle_{CMB} + \langle Q_y^2 \rangle_{CMB} + \langle U_x^2 \rangle_{CMB} + \langle U_y^2 \rangle_{CMB}. \quad (7)$$

In terms of the polarization power spectrum $C_l^{\tilde{P}\tilde{P}}$ it is given by

$$\sigma_{SP} = \int \frac{ldl}{2\pi} l^2 C_l^{\tilde{P}\tilde{P}}, \quad (8)$$

In the presence of lensing the average of equation (3) in the large scale limit becomes

$$\begin{aligned} \langle \mathcal{S}_P \rangle_{CMB} &= (1 - 2\kappa)\sigma_{SP} \\ \langle \mathcal{Q}_P \rangle_{CMB} &= -2\gamma_1\sigma_{SP} \\ \langle \mathcal{U}_P \rangle_{CMB} &= -2\gamma_2\sigma_{SP}, \end{aligned} \quad (9)$$

where the shear components γ_1 and γ_2 and convergence κ are defined as

$$\begin{aligned} \kappa &= -(\Phi_{xx} + \Phi_{yy})/2 \\ \gamma_1 &= -(\Phi_{xx} - \Phi_{yy})/2 \\ \gamma_2 &= -\Phi_{xy}. \end{aligned} \quad (10)$$

Physical interpretation of equation (9) is the following. Convergence κ stretches the images and makes the derivatives smaller, so $\langle \mathcal{S} \rangle_{CMB}$ is diminished by a factor proportional to κ . Similarly, shear produces anisotropy in the derivatives in the same way as in the images of distinct galaxies. To normalize the above expressions we introduce

$$\begin{aligned}
\mathcal{S}'_P &= -\frac{\mathcal{S}_P}{\sigma_{\mathcal{S}P}} + 1 \\
\mathcal{Q}'_P &= -\frac{\mathcal{Q}_P}{\sigma_{\mathcal{S}P}} \\
\mathcal{U}'_P &= -\frac{\mathcal{U}_P}{\sigma_{\mathcal{S}P}},
\end{aligned} \tag{11}$$

such that

$$\begin{aligned}
\langle \mathcal{S}'_P \rangle_{CMB} &= 2\kappa \\
\langle \mathcal{Q}'_P \rangle_{CMB} &= 2\gamma_1 \\
\langle \mathcal{U}'_P \rangle_{CMB} &= 2\gamma_2.
\end{aligned} \tag{12}$$

In the following we will only use these variables so we drop the primes from now on.

Instead of working with rotationally non-invariant quantities \mathcal{Q}_P and \mathcal{U}_P we combine them to form scalar field \mathcal{E}_P and pseudo-scalar \mathcal{B}_P . In the Fourier space these have the form

$$\begin{aligned}
\mathcal{E}_P(\mathbf{l}) &= \mathcal{Q}_P(\mathbf{l}) \cos(2\phi_{\mathbf{l}}) + \mathcal{U}_P(\mathbf{l}) \sin(2\phi_{\mathbf{l}}) \\
\mathcal{B}_P(\mathbf{l}) &= \mathcal{Q}_P(\mathbf{l}) \sin(2\phi_{\mathbf{l}}) - \mathcal{U}_P(\mathbf{l}) \cos(2\phi_{\mathbf{l}}),
\end{aligned} \tag{13}$$

where $\phi_{\mathbf{l}}$ is the azimuthal angle of the mode \mathbf{l} . In the Fourier space convergence and shear are related to each other through the relations

$$\gamma_1(\mathbf{l}) = \kappa(\mathbf{l}) \cos(2\phi_l) \quad \gamma_2(\mathbf{l}) = \kappa(\mathbf{l}) \sin(2\phi_l), \tag{14}$$

From equations (12), (13) and (14) it follows that

$$\begin{aligned}
\langle \mathcal{S}_P \rangle_{CMB} &= 2\kappa \\
\langle \mathcal{E}_P \rangle_{CMB} &= 2\kappa \\
\langle \mathcal{B}_P \rangle_{CMB} &= 0.
\end{aligned} \tag{15}$$

Thus the convergence κ can be reconstructed in two ways, either from \mathcal{S}_P or \mathcal{E}_P . Moreover, vanishing of \mathcal{B}_P on average can be helpful in indentifying the cosmological part of the signal or removing some foregrounds or other systematics.

To reconstruct the convergence power spectrum $C_l^{\kappa\kappa}$ we form its estimators

$$\hat{C}_l^{\mathcal{W}\mathcal{W}'} = \frac{1}{2} [\mathcal{W}(\mathbf{l})^* \mathcal{W}'(\mathbf{l}') + \mathcal{W}'(\mathbf{l}')^* \mathcal{W}(\mathbf{l})] \delta_{l'l'}, \tag{16}$$

where \mathcal{W} or \mathcal{W}' stand for \mathcal{S}_P , \mathcal{E}_P , \mathcal{S}_T or \mathcal{E}_T , with the first two obtained from polarization and the last two from temperature [9]. One can write the mean value of the estimator as

$$\langle \hat{C}_l^{\mathcal{W}\mathcal{W}'} \rangle_{CMB} = 4C_l^{\kappa\kappa} + N_l^{\mathcal{W}\mathcal{W}'}. \tag{17}$$

Here $N_l^{\mathcal{W}\mathcal{W}'}$ is a power spectrum of the noise arising from the intrinsic fluctuations in CMB temperature or polarization (or both for cross-correlation). This noise arises from the random nature of the CMB and has to be carefully examined to be properly subtracted from the estimated power spectrum $\hat{C}_l^{\mathcal{W}\mathcal{W}'}$ to get an unbiased convergence spectrum $C_l^{\kappa\kappa}$.

The noise power spectra can be computed analytically. First, we consider correlation functions between all the quantities $\tilde{\mathcal{S}}_P$, $\tilde{\mathcal{Q}}_P$, $\tilde{\mathcal{U}}_P$, $\tilde{\mathcal{S}}_T$, $\tilde{\mathcal{Q}}_T$ and $\tilde{\mathcal{U}}_T$. They are all defined as combinations of derivatives so using equations (3) and (11) results in the following expressions for the noise

$$\begin{aligned}
N^{\mathcal{S}_P\mathcal{S}_P}(\theta) &\equiv \langle \tilde{\mathcal{S}}_P(0) \tilde{\mathcal{S}}_P(\theta) \rangle_{CMB} \\
&= \frac{2}{\sigma_{\mathcal{S}P}^2} [(C_{xx}^{QQ})^2 + (C_{yy}^{QQ})^2 + (C_{xx}^{UU})^2 + (C_{yy}^{UU})^2 + 4(C_{xy}^{QU})^2] \\
N^{\mathcal{Q}_P\mathcal{Q}_P}(\theta) &\equiv \langle \tilde{\mathcal{Q}}_P(0) \tilde{\mathcal{Q}}_P(\theta) \rangle_{CMB} \\
&= \frac{2}{\sigma_{\mathcal{S}P}^2} [(C_{xx}^{QQ})^2 + (C_{yy}^{QQ})^2 + (C_{xx}^{UU})^2 + (C_{yy}^{UU})^2 - 4(C_{xy}^{QU})^2] \\
N^{\mathcal{U}_P\mathcal{U}_P}(\theta) &\equiv \langle \tilde{\mathcal{U}}_P(0) \tilde{\mathcal{U}}_P(\theta) \rangle_{CMB}
\end{aligned}$$

$$\begin{aligned}
&= \frac{4}{\sigma_{SP}^2} [C_{xx}^{QQ} C_{yy}^{QQ} + C_{xx}^{UU} C_{yy}^{UU} + 2(C_{xy}^{QU})^2] \\
N^{\mathcal{S}_P \mathcal{Q}_P}(\theta) &\equiv \langle \tilde{\mathcal{S}}_P(0) \tilde{\mathcal{Q}}_P(\theta) \rangle_{CMB} \\
&= \frac{2}{\sigma_{SP}^2} [(C_{xx}^{QQ})^2 - (C_{yy}^{QQ})^2 + (C_{xx}^{UU})^2 - (C_{yy}^{UU})^2] \\
N^{\mathcal{S}_T \mathcal{S}_P}(\theta) &\equiv \langle \tilde{\mathcal{S}}_T(0) \tilde{\mathcal{S}}_P(\theta) \rangle_{CMB} \\
&= \frac{2}{\sigma_{ST} \sigma_{SP}} [(C_{xx}^{TQ})^2 + (C_{yy}^{TQ})^2 + 2(C_{xy}^{TU})^2] \\
N^{\mathcal{Q}_T \mathcal{Q}_P}(\theta) &\equiv \langle \tilde{\mathcal{Q}}_T(0) \tilde{\mathcal{Q}}_P(\theta) \rangle_{CMB} \\
&= \frac{2}{\sigma_{ST} \sigma_{SP}} [(C_{xx}^{TQ})^2 + (C_{yy}^{TQ})^2 - 2(C_{xy}^{TU})^2] \\
N^{\mathcal{U}_T \mathcal{U}_P}(\theta) &\equiv \langle \tilde{\mathcal{U}}_T(0) \tilde{\mathcal{U}}_P(\theta) \rangle_{CMB} \\
&= \frac{4}{\sigma_{ST} \sigma_{SP}} [C_{xx}^{TQ} C_{yy}^{TQ} + (C_{xy}^{TU})^2] \\
N^{\mathcal{S}_T \mathcal{Q}_P}(\theta) &\equiv \langle \tilde{\mathcal{S}}_T(0) \tilde{\mathcal{Q}}_P(\theta) \rangle_{CMB} \\
&= \frac{2}{\sigma_{ST} \sigma_{SP}} [(C_{xx}^{TQ})^2 - (C_{yy}^{TQ})^2]. \tag{18}
\end{aligned}$$

Those for temperature are given in [9] and will not be repeated here. The correlation functions C_{xy}^{XY} are given in the Appendix. Equations (18) together with equations (A2) contain all the necessary information for noise estimate. In figure 1 we show correlation functions for polarization and cross-correlation between temperature and polarization. We assume throughout that the underlying model is the concordance model [10] with $\Omega_b = 0.04$, $\Omega_m = 0.33$, $\Omega_\Lambda = 0.63$, $h = 0.65$ and $n_s = 1$. As discussed in [5] other viable models give comparable results for signal to noise. For this model the correlation length for polarization is $\xi_{PP} \sim 0.07^\circ$, while for cross-correlation $\xi_{TP} \sim 0.1^\circ$ and for temperature $\xi_{TT} \sim 0.15^\circ$. Each patch of size ξ^2 is roughly independent and decreasing ξ by a factor of 2 therefore increases by 4 number of independent patches. Since on large scales CMB noise behaves roughly as a white noise this reduces the noise level by corresponding factor. This implies that if we could observe polarization with perfect resolution it would give significantly larger signal to noise than temperature alone. However, since polarization has a weaker signal than temperature this advantage becomes possible only for very sensitive detectors and small beams, as discussed below in more detail.

The noise power spectra can be obtained from the real space correlations using the following expressions [13]

$$\begin{aligned}
N_l^{\mathcal{S}_A \mathcal{S}_B} &= 2\pi \int \theta d\theta N^{\mathcal{S}_A \mathcal{S}_B}(\theta) J_0(l\theta) \\
N_l^{\mathcal{E}_A \mathcal{E}_B} &= \pi \int \theta d\theta \{ [N^{\mathcal{Q}_A \mathcal{Q}_B}(\theta) + N^{\mathcal{U}_A \mathcal{U}_B}(\theta)] J_0(l\theta) + [N^{\mathcal{Q}_A \mathcal{Q}_B}(\theta) - N^{\mathcal{U}_A \mathcal{U}_B}(\theta)] J_4(l\theta) \} \\
N_l^{\mathcal{B}_A \mathcal{B}_B} &= \pi \int \theta d\theta \{ [N^{\mathcal{Q}_A \mathcal{Q}_B}(\theta) + N^{\mathcal{U}_A \mathcal{U}_B}(\theta)] J_0(l\theta) - [N^{\mathcal{Q}_A \mathcal{Q}_B}(\theta) - N^{\mathcal{U}_A \mathcal{U}_B}(\theta)] J_4(l\theta) \} \\
N_l^{\mathcal{S}_A \mathcal{E}_B} &= 2\pi \int \theta d\theta N^{\mathcal{S}_A \mathcal{Q}_B}(\theta) J_2(l\theta), \tag{19}
\end{aligned}$$

where A and B stand for T or P . From this one obtains the CMB noise power spectra

$$\begin{aligned}
N_l^{\mathcal{S}_P \mathcal{S}_P} &= \frac{\pi}{2\sigma_{SP}^2} \int \theta d\theta \{ 2(C_0^{\tilde{P}\tilde{P}})^2 + 3(C_2^{\tilde{P}\tilde{P}})^2 + 2(C_4^{\tilde{P}\tilde{P}})^2 + (C_6^{\tilde{P}\tilde{P}})^2 \} J_0(l\theta) \\
N_l^{\mathcal{E}_P \mathcal{E}_P} &= \frac{\pi}{\sigma_{SP}^2} \int \theta d\theta \{ (C_0^{\tilde{P}\tilde{P}})^2 + (C_4^{\tilde{P}\tilde{P}})^2 \} J_0(l\theta) + \{ (C_2^{\tilde{P}\tilde{P}})^2 + 2C_2^{\tilde{P}\tilde{P}} C_6^{\tilde{P}\tilde{P}} \} J_4(l\theta) \\
N_l^{\mathcal{B}_P \mathcal{B}_P} &= \frac{\pi}{\sigma_{SP}^2} \int \theta d\theta \{ (C_0^{\tilde{P}\tilde{P}})^2 + (C_4^{\tilde{P}\tilde{P}})^2 \} J_0(l\theta) - \{ (C_2^{\tilde{P}\tilde{P}})^2 + 2C_2^{\tilde{P}\tilde{P}} C_6^{\tilde{P}\tilde{P}} \} J_4(l\theta) \\
N_l^{\mathcal{S}_P \mathcal{E}_P} &= -\frac{\pi}{\sigma_{SP}^2} \int \theta d\theta \{ 2C_0^{\tilde{P}\tilde{P}} C_2^{\tilde{P}\tilde{P}} + C_2^{\tilde{P}\tilde{P}} C_4^{\tilde{P}\tilde{P}} + C_4^{\tilde{P}\tilde{P}} C_6^{\tilde{P}\tilde{P}} \} J_2(l\theta) \\
N_l^{\mathcal{S}_T \mathcal{S}_P} &= \frac{\pi}{\sigma_{ST} \sigma_{SP}} \int \theta d\theta \{ (C_0^{\tilde{T}\tilde{P}})^2 + 2(C_2^{\tilde{T}\tilde{P}})^2 + 4(C_4^{\tilde{T}\tilde{P}})^2 \} J_0(l\theta)
\end{aligned}$$

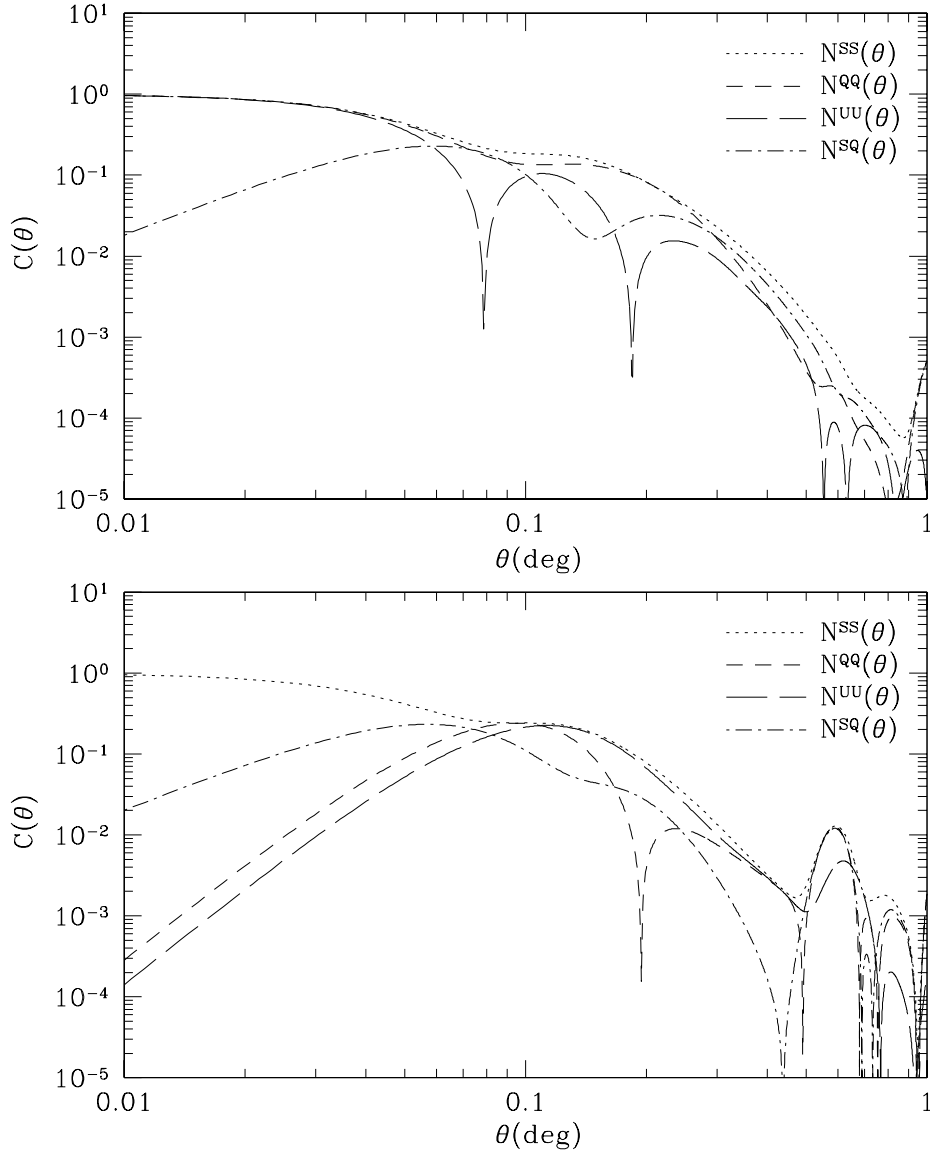


FIG. 1. The upper panel shows auto-correlation functions for polarization $N^{S_P S_P}(\theta)$, $N^{Q_P Q_P}(\theta)$, $N^{U_P U_P}(\theta)$ and $N^{S_P Q_P}(\theta)$. The lower panel shows the cross-correlations $N^{S_T S_P}(\theta)$, $N^{Q_T Q_P}(\theta)$, $N^{U_T U_P}(\theta)$ and $N^{S_T Q_P}(\theta)$. Both plots are for the cosmological concordance model (see text) and without detector noise.

$$\begin{aligned}
N_l^{\mathcal{E}_T \mathcal{E}_P} &= \frac{2\pi}{\sigma_{ST} \sigma_{SP}} \int \theta d\theta \left\{ (C_2^{\tilde{T}\tilde{P}})^2 J_0(l\theta) + C_0^{\tilde{T}\tilde{P}} C_4^{\tilde{T}\tilde{P}} J_4(l\theta) \right\} \\
N_l^{\mathcal{B}_T \mathcal{B}_P} &= \frac{2\pi}{\sigma_{ST} \sigma_{SP}} \int \theta d\theta \left\{ (C_2^{\tilde{T}\tilde{P}})^2 J_0(l\theta) - C_0^{\tilde{T}\tilde{P}} C_4^{\tilde{T}\tilde{P}} J_4(l\theta) \right\} \\
N_l^{\mathcal{S}_T \mathcal{E}_P} &= -\frac{2\pi}{\sigma_{ST} \sigma_{SP}} \int \theta d\theta \left\{ C_0^{\tilde{T}\tilde{P}} + C_4^{\tilde{T}\tilde{P}} \right\} C_2^{\tilde{T}\tilde{P}} J_2(l\theta)
\end{aligned} \tag{20}$$

We do not need to consider spectra containing \mathcal{B}_T or \mathcal{B}_P as these pseudo-scalar quantities do not correlate with scalars. Fig. 2 shows noise power spectra for polarization and cross-correlation. The most visible feature is the white noise behavior on large scales, which confirms that derivatives of temperature and Stokes parameters are almost uncorrelated on scales above a fraction of a degree.

Let us consider now the power spectra in the limit of low l . Utilizing of the Bessel functions properties in this limit and their orthonormality relations we obtain from equation (20) the following limits

$$\lim_{l \rightarrow 0} N_l^{\mathcal{S}_P \mathcal{S}_P} = 4\pi \frac{\int l^5 dl (C_l^{\tilde{P}\tilde{P}})^2}{(\int l^3 dl C_l^{\tilde{P}\tilde{P}})^2} \tag{21}$$

$$\lim_{l \rightarrow 0} N_l^{\mathcal{E}_P \mathcal{E}_P} = \lim_{l \rightarrow 0} N_l^{\mathcal{B}_P \mathcal{B}_P} = \frac{1}{2} \lim_{l \rightarrow 0} N_l^{\mathcal{S}_P \mathcal{S}_P} \tag{21}$$

$$\lim_{l \rightarrow 0} N_l^{\mathcal{S}_P \mathcal{E}_P} = 0$$

$$\lim_{l \rightarrow 0} N_l^{\mathcal{S}_T \mathcal{S}_P} = 4\pi \frac{\int l^5 dl (C_l^{\tilde{T}\tilde{P}})^2}{\int l^3 dl C_l^{\tilde{T}\tilde{T}} \int l^3 dl C_l^{\tilde{P}\tilde{P}}} \tag{22}$$

$$\lim_{l \rightarrow 0} N_l^{\mathcal{E}_T \mathcal{E}_P} = \lim_{l \rightarrow 0} N_l^{\mathcal{B}_T \mathcal{B}_P} = \frac{1}{2} \lim_{l \rightarrow 0} N_l^{\mathcal{S}_T \mathcal{S}_P} \tag{22}$$

$$\lim_{l \rightarrow 0} N_l^{\mathcal{S}_T \mathcal{E}_P} = 0.$$

The power spectra presented in the fig. 2 confirm this large scale behavior. It is worth noting that the noise for \mathcal{S} variables is two times higher than for \mathcal{E} and \mathcal{B} , although normalized variances of $\tilde{\mathcal{S}}_P$, $\tilde{\mathcal{Q}}_P$ and $\tilde{\mathcal{U}}_P$ are all the same. This is because of the spin nature of $\tilde{\mathcal{Q}}_P$ and $\tilde{\mathcal{U}}_P$. The implication of this is that the reconstructed convergence power spectrum will have the noise amplitude two times lower when we use \mathcal{E}_P instead of \mathcal{S}_P .

When we have quantified the intrinsic CMB noise we can use equation (17) to obtain the best estimate for $\hat{C}_l^{\kappa\kappa}$ from observations. In addition, we also need to determine the error on the estimated power spectrum $\hat{C}_l^{\mathcal{W}\mathcal{W}'}$. To proceed analytically we make an additional assumption that Fourier transforms of quantities \mathcal{S}_P , \mathcal{E}_P , \mathcal{S}_T and \mathcal{E}_T are Gaussian distributed. From simulations presented in [9] this seems to be a good approximation on large scales, where a single long wavelength mode receives contribution from many almost independent structures in real space and the central limit theorem makes them almost Gaussian. In general, from \mathcal{S}_T , \mathcal{E}_T , \mathcal{S}_P and \mathcal{E}_P we can construct 10 estimators of $C_l^{\kappa\kappa}$, 3 for the temperature field, 3 for polarization and 4 for cross-correlation. Under these assumptions we obtain the elements of the covariance matrices of the polarization and cross-correlation estimators

$$\text{Var} \left(\hat{C}_l^{\mathcal{S}_A \mathcal{S}_B} \right) = \frac{1}{2l+1} \left[(4C_l^{\kappa\kappa} + N_l^{\mathcal{S}_A \mathcal{S}_B})^2 + (4C_l^{\kappa\kappa} + N_l^{\mathcal{S}_A \mathcal{S}_A})(4C_l^{\kappa\kappa} + N_l^{\mathcal{S}_B \mathcal{S}_B}) \right] \tag{23}$$

$$\text{Var} \left(\hat{C}_l^{\mathcal{E}_A \mathcal{E}_B} \right) = \frac{1}{2l+1} \left[(4C_l^{\kappa\kappa} + N_l^{\mathcal{E}_A \mathcal{E}_B})^2 + (4C_l^{\kappa\kappa} + N_l^{\mathcal{E}_A \mathcal{E}_A})(4C_l^{\kappa\kappa} + N_l^{\mathcal{E}_B \mathcal{E}_B}) \right] \tag{24}$$

$$\text{Var} \left(\hat{C}_l^{\mathcal{B}_A \mathcal{B}_B} \right) = \frac{1}{2l+1} \left[(N_l^{\mathcal{B}_A \mathcal{B}_B})^2 + N_l^{\mathcal{B}_A \mathcal{B}_A} N_l^{\mathcal{B}_B \mathcal{B}_B} \right] \tag{25}$$

$$\text{Var} \left(\hat{C}_l^{\mathcal{S}_A \mathcal{E}_B} \right) = \frac{1}{2l+1} \left[(4C_l^{\kappa\kappa} + N_l^{\mathcal{S}_A \mathcal{E}_B})^2 + (4C_l^{\kappa\kappa} + N_l^{\mathcal{S}_A \mathcal{S}_A})(4C_l^{\kappa\kappa} + N_l^{\mathcal{E}_B \mathcal{E}_B}) \right] \tag{26}$$

$$\text{Var} \left(\hat{C}_l^{\mathcal{E}_A \mathcal{S}_B} \right) = \frac{1}{2l+1} \left[(4C_l^{\kappa\kappa} + N_l^{\mathcal{E}_A \mathcal{S}_B})^2 + (4C_l^{\kappa\kappa} + N_l^{\mathcal{E}_A \mathcal{E}_A})(4C_l^{\kappa\kappa} + N_l^{\mathcal{S}_B \mathcal{S}_B}) \right] \tag{27}$$

$$\text{Cov} \left(\hat{C}_l^{\mathcal{S}_A \mathcal{S}_B}, \hat{C}_l^{\mathcal{E}_A \mathcal{E}_B} \right) = \frac{1}{2l+1} \left[(4C_l^{\kappa\kappa} + N_l^{\mathcal{S}_A \mathcal{E}_B})^2 + (4C_l^{\kappa\kappa} + N_l^{\mathcal{S}_A \mathcal{E}_A})(4C_l^{\kappa\kappa} + N_l^{\mathcal{S}_B \mathcal{E}_B}) \right] \tag{28}$$

$$\text{Cov} \left(\hat{C}_l^{\mathcal{S}_A \mathcal{S}_B}, \hat{C}_l^{\mathcal{S}_A \mathcal{E}_B} \right) = \frac{1}{2l+1} \left[(4C_l^{\kappa\kappa} + N_l^{\mathcal{S}_A \mathcal{S}_B})(4C_l^{\kappa\kappa} + N_l^{\mathcal{S}_A \mathcal{E}_B}) + (4C_l^{\kappa\kappa} + N_l^{\mathcal{S}_A \mathcal{S}_A})(4C_l^{\kappa\kappa} + N_l^{\mathcal{S}_B \mathcal{E}_B}) \right] \tag{29}$$

$$\text{Cov} \left(\hat{C}_l^{\mathcal{E}_A \mathcal{E}_B}, \hat{C}_l^{\mathcal{S}_A \mathcal{E}_B} \right) = \frac{1}{2l+1} \left[(4C_l^{\kappa\kappa} + N_l^{\mathcal{E}_A \mathcal{E}_B})(4C_l^{\kappa\kappa} + N_l^{\mathcal{S}_A \mathcal{E}_B}) + (4C_l^{\kappa\kappa} + N_l^{\mathcal{S}_A \mathcal{E}_A})(4C_l^{\kappa\kappa} + N_l^{\mathcal{E}_B \mathcal{E}_B}) \right] \tag{30}$$

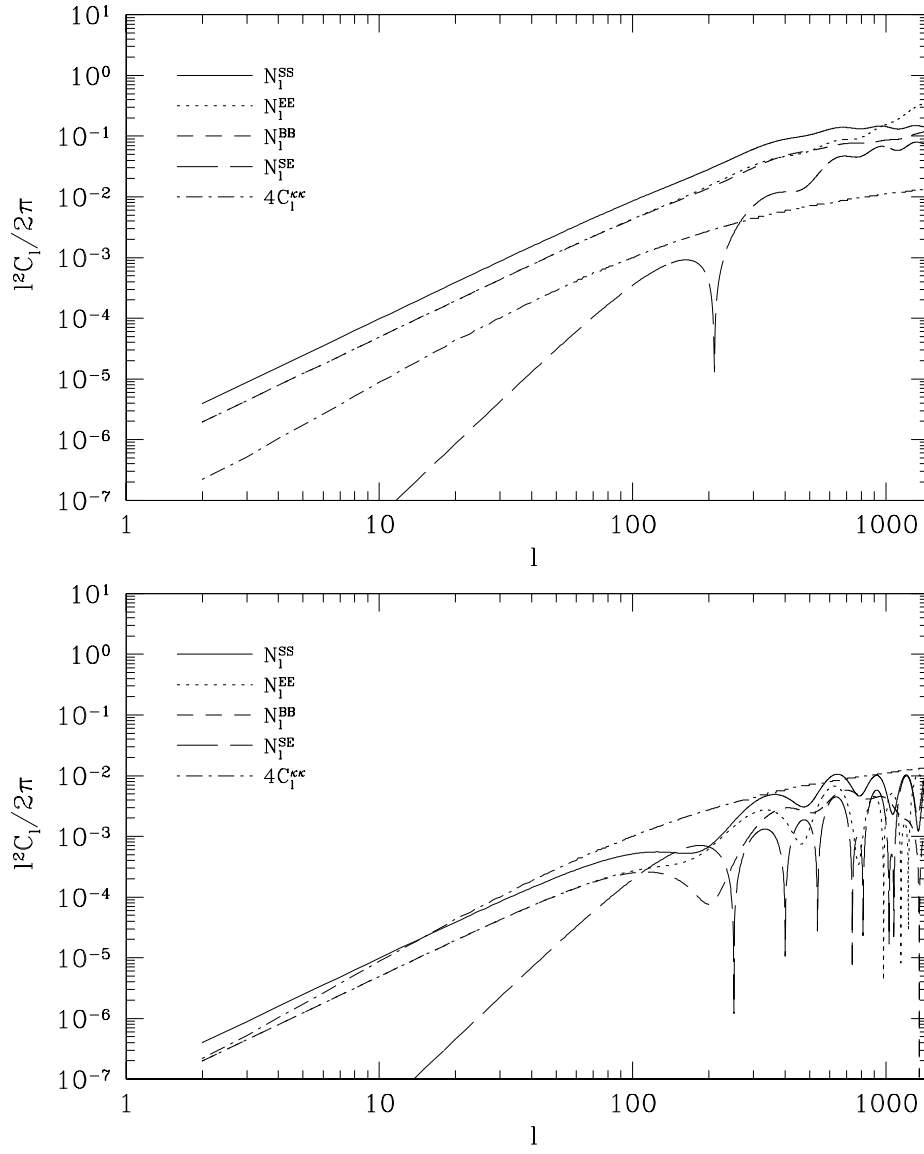


FIG. 2. In the upper panel there are noise power spectra for polarization $N_l^{S_P S_P}$, $N_l^{\mathcal{E}_P \mathcal{E}_P}$, $N_l^{B_P B_P}$ and $N_l^{S_P \mathcal{E}_P}$, yet in the lower panel for the cross-correlation $N_l^{S_T S_P}$, $N_l^{\mathcal{E}_T \mathcal{E}_P}$, $N_l^{B_T B_P}$ and $N_l^{S_T \mathcal{E}_P}$. They are coupled with correlation functions presented in fig.1 via equations (19).

$$\text{Cov} \left(\hat{C}_l^{\mathcal{E}_A \mathcal{S}_B}, \hat{C}_l^{\mathcal{S}_A \mathcal{E}_B} \right) = \frac{1}{2l+1} \left[(4C_l^{\kappa\kappa} + N_l^{\mathcal{E}_A \mathcal{E}_B})(4C_l^{\kappa\kappa} + N_l^{\mathcal{S}_A \mathcal{S}_B}) + (4C_l^{\kappa\kappa} + N_l^{\mathcal{S}_A \mathcal{E}_A})(4C_l^{\kappa\kappa} + N_l^{\mathcal{S}_B \mathcal{E}_B}) \right] \quad (31)$$

$$\text{Cov} \left(\hat{C}_l^{\mathcal{E}_A \mathcal{S}_B}, \hat{C}_l^{\mathcal{S}_A \mathcal{S}_B} \right) = \frac{1}{2l+1} \left[(4C_l^{\kappa\kappa} + N_l^{\mathcal{E}_A \mathcal{S}_A})(4C_l^{\kappa\kappa} + N_l^{\mathcal{S}_B \mathcal{S}_B}) + (4C_l^{\kappa\kappa} + N_l^{\mathcal{E}_A \mathcal{S}_B})(4C_l^{\kappa\kappa} + N_l^{\mathcal{S}_A \mathcal{S}_B}) \right] \quad (32)$$

$$\text{Cov} \left(\hat{C}_l^{\mathcal{E}_A \mathcal{S}_B}, \hat{C}_l^{\mathcal{E}_A \mathcal{E}_B} \right) = \frac{1}{2l+1} \left[(4C_l^{\kappa\kappa} + N_l^{\mathcal{E}_A \mathcal{E}_B})(4C_l^{\kappa\kappa} + N_l^{\mathcal{S}_B \mathcal{E}_A}) + (4C_l^{\kappa\kappa} + N_l^{\mathcal{E}_A \mathcal{E}_A})(4C_l^{\kappa\kappa} + N_l^{\mathcal{S}_B \mathcal{E}_B}) \right] \quad (33)$$

where A and B stand for T or P again.

To assess the variance of the overall estimator $\hat{C}_l^{\kappa\kappa}$ that is a combination of three estimators in the case of polarization and four in the case of cross-correlation (eq. 17) we treat our variables \mathcal{S}_T , \mathcal{S}_P , \mathcal{E}_T and \mathcal{E}_P as Gaussian. Using the Fisher information matrix we can derive the desired variances [11]

$$\mathcal{F}_{ij} = \frac{1}{2} \text{Tr} \left[\text{Cov}^{-1}(\mathcal{W}, \mathcal{W}') \frac{\partial \text{Cov}(\mathcal{W}, \mathcal{W}')}{\partial s_i} \text{Cov}^{-1}(\mathcal{W}, \mathcal{W}') \frac{\partial \text{Cov}(\mathcal{W}, \mathcal{W}')}{\partial s_j} \right]. \quad (34)$$

The inverse of the Fisher matrix gives the covariance matrix. The Fisher matrix is one dimensional and relevant derivatives are taken with respect to $C_l^{\kappa\kappa}$. We find the following expression for variance of the $\hat{C}_l^{\kappa\kappa}$ estimator when we take into account only polarization information

$$\text{Var} \left(\hat{C}_l^{\kappa\kappa} \right)_{PP} = \frac{1}{8(2l+1)} \frac{\left[C_l^{\mathcal{S}_P \mathcal{S}_P} C_l^{\mathcal{E}_P \mathcal{E}_P} - \left(C_l^{\mathcal{S}_P \mathcal{E}_P} \right)^2 \right]^2}{\left[C_l^{\mathcal{S}_P \mathcal{S}_P} + C_l^{\mathcal{E}_P \mathcal{E}_P} - 2C_l^{\mathcal{S}_P \mathcal{E}_P} \right]^2} \quad (35)$$

Similarly, using the cross-correlation variables only the variance is

$$\text{Var} \left(\hat{C}_l^{\kappa\kappa} \right)_{TP} = \frac{1}{8(2l+1)} \frac{\left[C_l^{\mathcal{S}_T \mathcal{S}_T} C_l^{\mathcal{E}_T \mathcal{E}_T} - \left(C_l^{\mathcal{S}_T \mathcal{E}_T} \right)^2 \right] \left[C_l^{\mathcal{S}_P \mathcal{S}_P} C_l^{\mathcal{E}_P \mathcal{E}_P} - \left(C_l^{\mathcal{S}_P \mathcal{E}_P} \right)^2 \right]}{\left[C_l^{\mathcal{S}_T \mathcal{S}_T} + C_l^{\mathcal{E}_T \mathcal{E}_T} - 2C_l^{\mathcal{S}_T \mathcal{E}_T} \right]^2 \left[C_l^{\mathcal{S}_P \mathcal{S}_P} + C_l^{\mathcal{E}_P \mathcal{E}_P} - 2C_l^{\mathcal{S}_P \mathcal{E}_P} \right]^2}, \quad (36)$$

where we have dropped the cross-correlation terms $C^{\mathcal{W}_T \mathcal{W}_P}$ which are much smaller than the diagonal terms in the large scale limit. For an experiment like MAP or Planck we will have $N^{\mathcal{S}_P \mathcal{S}_P} \gg N^{\mathcal{S}_T \mathcal{S}_T} \gg N^{\mathcal{S}_T \mathcal{S}_P}$ and the same for other combinations of \mathcal{S}_T , \mathcal{E}_T , \mathcal{S}_P , \mathcal{E}_P , as can be seen from the noise spectra in figure 4. Only for a significantly more sensitive detector will the three noise spectra become comparable in which case, as argued above, polarization noise power spectrum will become smaller than that of the temperature. For this reason we provide separately the information from polarization and from temperature polarization cross-correlation. In addition, the cosmic variance term proportional to $4C_l^{\kappa\kappa}$ is also much smaller than the CMB intrinsic noise contribution and can be dropped. The main source of errors is then the intrinsic CMB noise. In the large scale limit $N^{\mathcal{S}_P \mathcal{E}_P}$ is more than an order of magnitude less than $N^{\mathcal{S}_P \mathcal{S}_P}$, $N^{\mathcal{E}_P \mathcal{E}_P}$ or $N^{\mathcal{B}_P \mathcal{B}_P}$ that implies we can neglect that term in the covariances. These approximations lead to a diagonal form of covariance matrices that can be written as

$$\text{Var} \left(\hat{C}_l^{\kappa\kappa} \right)_{PP} = 8(2l+1) \left[\frac{1}{(C_l^{\mathcal{S}_T \mathcal{S}_T})^2} + \frac{1}{(C_l^{\mathcal{E}_T \mathcal{E}_T})^2} + \frac{2}{C_l^{\mathcal{S}_T \mathcal{S}_T} C_l^{\mathcal{E}_T \mathcal{E}_T}} \right] \quad (37)$$

$$\text{Var} \left(\hat{C}_l^{\kappa\kappa} \right)_{TP} = 8(2l+1) \left[\frac{1}{C_l^{\mathcal{S}_T \mathcal{S}_T} C_l^{\mathcal{S}_P \mathcal{S}_P} + \frac{1}{C_l^{\mathcal{E}_T \mathcal{E}_T} C_l^{\mathcal{E}_P \mathcal{E}_P} + \frac{1}{C_l^{\mathcal{S}_T \mathcal{S}_T} C_l^{\mathcal{E}_P \mathcal{E}_P} + \frac{1}{C_l^{\mathcal{E}_T \mathcal{E}_T} C_l^{\mathcal{S}_P \mathcal{S}_P}} \right] \quad (38)$$

The minimum variance combination of these estimators in the large scale limit is for polarization

$$\langle 4\hat{C}_l^{\kappa\kappa} \rangle = \frac{1}{9} \left(\langle \hat{C}_l^{\mathcal{S}_P \mathcal{S}_P} \rangle - N_l^{\mathcal{S}_P \mathcal{S}_P} \right) + \frac{4}{9} \left(\langle \hat{C}_l^{\mathcal{E}_P \mathcal{E}_P} \rangle - N_l^{\mathcal{E}_P \mathcal{E}_P} \right) + \frac{4}{9} \left(\langle \hat{C}_l^{\mathcal{S}_P \mathcal{E}_P} \rangle - N_l^{\mathcal{S}_P \mathcal{E}_P} \right) \quad (39)$$

and for cross-correlation

$$\langle 4\hat{C}_l^{\kappa\kappa} \rangle = \frac{1}{9} \left(\langle \hat{C}_l^{\mathcal{S}_T \mathcal{S}_P} \rangle - N_l^{\mathcal{S}_T \mathcal{S}_P} \right) + \frac{4}{9} \left(\langle \hat{C}_l^{\mathcal{E}_T \mathcal{E}_P} \rangle - N_l^{\mathcal{E}_T \mathcal{E}_P} \right) + \frac{2}{9} \left(\langle \hat{C}_l^{\mathcal{S}_T \mathcal{E}_P} \rangle - N_l^{\mathcal{S}_T \mathcal{E}_P} \right) + \frac{2}{9} \left(\langle \hat{C}_l^{\mathcal{E}_T \mathcal{S}_P} \rangle - N_l^{\mathcal{E}_T \mathcal{S}_P} \right) \quad (40)$$

In the limit $l \rightarrow 0$ variances of these overall estimators can be written as

$$\text{Var} \left(4\hat{C}_l^{\kappa\kappa} \right)_{PP} = \frac{2}{9(2l+1)} (N_l^{\mathcal{S}_P\mathcal{S}_P})^2 \quad (41)$$

$$\text{Var} \left(4\hat{C}_l^{\kappa\kappa} \right)_{TP} = \frac{1}{9(2l+1)} N_l^{\mathcal{S}_T\mathcal{S}_T} N_l^{\mathcal{S}_P\mathcal{S}_P} \quad (42)$$

These expressions show that if $N_l^{\mathcal{S}_T\mathcal{S}_T} \ll N_l^{\mathcal{S}_P\mathcal{S}_P}$ then it will be the cross-correlation that will add most of polarization information to $C_l^{\kappa\kappa}$. This information increase will be small compared to the information obtained from the temperature alone, but may still provide important independent confirmation. If $N_l^{\mathcal{S}_T\mathcal{S}_T} \sim N_l^{\mathcal{S}_P\mathcal{S}_P}$ polarization provides as much information to $C_l^{\kappa\kappa}$ as temperature. In further considerations we will use the complete expressions for respective variances without the above approximations.

Another consequence of the intrinsic CMB fluctuations is that we cannot recover the convergence from the individual structures, because the coherence length of CMB is too large. We will show that it is still possible to measure the convergence in a statistical sense, by averaging over many Fourier modes to extract the power spectrum. We will determine the signal to noise for various detector sensitivities in the following section.

III. CONVERGENCE FROM OBSERVATIONS

Before computing the expected signal to noise for future missions we need to include the effect of detector noise and angular resolution on extracting the convergence power spectrum. Both of these have been discussed in [9] and the expressions derived there can be applied to polarization as well.

To quantify the influence of the detector beam on measured Stokes parameters one introduces a filter function $F(\boldsymbol{\theta})$, which describes the detector beam filtering of the data. The Stokes parameters are convolved with this function

$$X_a(\boldsymbol{\theta}) = \int F(\boldsymbol{\theta} - \boldsymbol{\theta}') X_a(\boldsymbol{\theta}') d^2\boldsymbol{\theta}' \quad (43)$$

where X stands for Stokes parameters Q or U . Using equation (2) and Fourier decomposition equation (43) becomes

$$X_a(\boldsymbol{\theta}) = \frac{1}{(2\pi)^2} \int d^2\mathbf{l} F(l) X_a(\mathbf{l}) e^{i\mathbf{l}\cdot\boldsymbol{\theta}} + \frac{1}{(2\pi)^4} \int d^2\mathbf{l} \int d^2\mathbf{q} F(|\mathbf{l} + \mathbf{q}|) X_b(\mathbf{l}) \Phi_{ab}(\mathbf{q}) e^{i(\mathbf{l} + \mathbf{q})\cdot\boldsymbol{\theta}}. \quad (44)$$

In the presence of filter $F(\boldsymbol{\theta})$ it follows from equations (3) and (44)

$$\langle \mathcal{S}_P(\boldsymbol{\theta}) \rangle_{CMB} = \frac{1}{(2\pi)^2} \int d^2\mathbf{l} F^2(l) l^2 C_l^{\bar{P}\bar{P}} \left[1 - \frac{1}{(2\pi)^2} \int d^2\mathbf{q} 2\kappa(\mathbf{q}) W_P(\mathbf{q}) e^{i\mathbf{q}\cdot\boldsymbol{\theta}} \right]. \quad (45)$$

We introduced the window function $W_P(\mathbf{q})$ to describe the effect of the detector beam on the convergence. It has the form

$$W_P(q) = \frac{\int d^2\mathbf{l} F(l) F(|\mathbf{l} + \mathbf{q}|) l^2 C_l^{\bar{P}\bar{P}}}{\int d^2\mathbf{l} F^2(l) l^2 C_l^{\bar{P}\bar{P}}}. \quad (46)$$

We see that $W_P(q) \rightarrow 1$ for $q \rightarrow 0$ independently of the explicit form of the filter. Thus for large scales we reconstruct the convergence power spectrum without beam degradation. More generally, the relation between the observables and underlying convergence is

$$\langle \mathcal{S}_P(\mathbf{l}) \rangle_{CMB} = \langle \mathcal{E}_P(\mathbf{l}) \rangle_{CMB} = 2\kappa(\mathbf{l}) W_P(l) \quad (47)$$

Window for Planck in the case of polarization and temperature is shown in fig. 3a. Just like in the case of temperature [9] we remove small scale modes with $l > l_{cut}$ where detector noise exceeds primary signal (see below). At $l \sim 300$ the beam already reduces the sensitivity by 50%. Ten times more sensitive detectors would significantly extend the range of sensitivity and would be able to measure polarization spectrum up to approximately $l \approx 2000$. The window for such a detector is also shown in fig. 3a.

In the presence of the beam smoothing the equation (17) is rewritten for polarization in the form

$$\langle \hat{C}_l^{\mathcal{W}\mathcal{W}'} \rangle_{CMB} = 4W_P^2(l) C_l^{\kappa\kappa} + N_l^{\mathcal{W}\mathcal{W}'}, \quad (48)$$

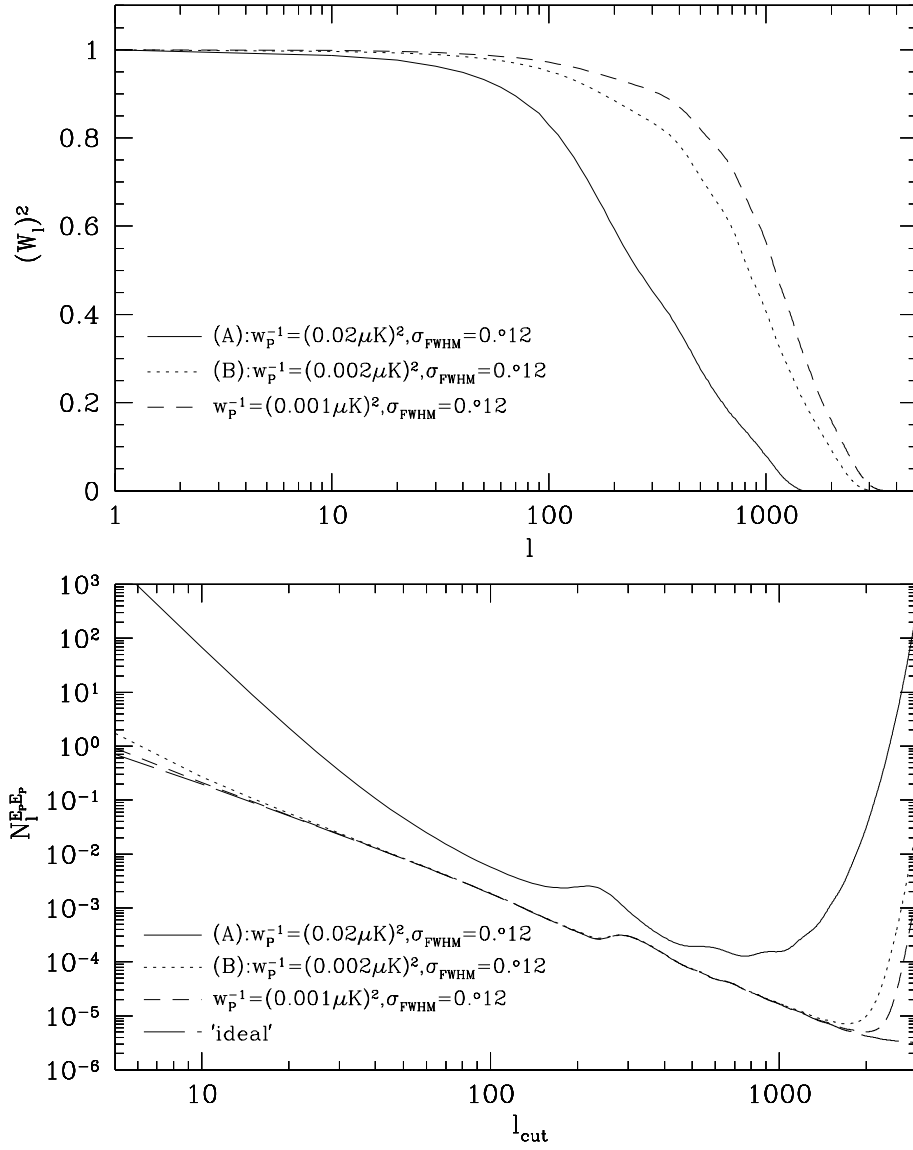


FIG. 3. In the upper panel square of the window function for a few detector configurations using the optimal l_{cut} is shown. In the lower panel $N_l^{E_P E_P}$ is shown as a function of l_{cut} using the white noise approximation. Detector (A) is for current Planck proposal. Increasing the detector sensitivity by another order of magnitude, as could be achieved by post-Planck generation of CMB satellites, would bring the noise level close to the ideal case.

while for cross-correlation its form is

$$\langle \hat{C}_l^{WW'} \rangle_{CMB} = 4W_T(l)W_P(l)C_l^{\kappa\kappa} + N_l^{WW'}. \quad (49)$$

Note that to assess the noise power spectrum we need to measure the CMB polarization, temperature and cross-correlation spectrum first.

Detector noise affects the results through the increase of the CMB correlation length. The detector noise spectrum w_P^{-1} is taken as a white noise in the considered range and is related to the pixel noise and its solid angle size through $w_P^{-1} = \sigma_{\text{pixel}}^2 \Omega_{\text{pixel}}$ and similarly for temperature. Planck for example is expected to have the resolution of $\sigma_{\text{FWHM}} = 0.12^\circ$ and the noise $w_P^{-1} = (0.02)^2 (\mu K)^2$. Individual structures on small scales are dominated by noise and cannot be observed, hence cannot be used to reconstruct convergence so it is best to remove them. We remove them by filtering the data on scale corresponding to the scale where noise and signal power spectra are equal, which in Fourier space defines some value for l_{cut} . In fact, for the white noise approximation the spectra have the form presented in equation (21) which for polarization gives

$$N_l^{\mathcal{E}_P \mathcal{E}_P} = 2\pi \frac{\int_0^{l_{\text{cut}}} l^5 dl (C_l^{\bar{P}\bar{P}} + w_P^{-1} e^{l^2 \sigma_b^2})^2}{(\int l^3 dl C_l^{\bar{P}\bar{P}})^2}. \quad (50)$$

This can be used to determine l_{cut} which minimizes the noise, at least on large scales where the approximation is valid. In fig. 3b are shown a few examples of the detector configurations as a function of l_{cut} . For non-zero detector noise the curves have minima in l_{cut} above which noise increases rapidly as expected. Small l_{cut} filters out real CMB structure and increase the correlation length, thus increasing the level of noise. Once l_{cut} becomes too large the filtering scale is too small and small scale power is dominated by noise. This does not have any information on the lensing signal and increase the overall noise level again. The optimal value for l_{cut} is found in between these two regimes and agrees well with the value defined where the noise and signal power spectra in CMB are equal.

Figure 4 gives the expected temperature, polarization and cross-correlation noise spectra for Planck as well as the expected convergence power spectrum. Noise is always several times larger than the expected signal so extraction of $C_l^{\kappa\kappa}$ is possible only in the statistical sense, by averaging over many multipoles. In case of polarization the noise is about two orders of magnitude larger than the signal. This means that for Planck one would need to average over 2×10^4 modes to obtain $S/N \sim 1$. This is further reduced by the effect of the window. A more accurate estimate of expected signal to noise can be obtained by combining the information from all multipoles and form the optimal estimator [7]. This gives

$$\left(\frac{S}{N} \right)_{AB} = \left(f_{\text{sky}} \sum_l \frac{W_A^2(l) W_B^2(l) \langle \hat{C}_l^{\kappa\kappa} \rangle^2}{\text{Var}(\hat{C}_l^{\kappa\kappa})} \right)^{1/2} \quad (51)$$

where f_{sky} is the fraction of the sky covered, here taken to be 0.7. Results are shown in the fig. 5. For Planck the signal to noise ratio for polarization reaches only $(S/N)_{PP} \sim 1$ when we take into account about 400 multipoles and does not increase beyond that. So the detection of the convergence by Planck from the polarization measurements is not really possible, unless the signal in convergence is significantly higher than assumed here. The case of the cross-correlation is more promising because of lower noise in temperature. Here we find it is possible to get $(S/N)_{TP} \sim 5$ from $l < 400$. More promising numbers are found if we increase the detector sensitivity by a factor of several, which could only be achieved from the next generation of CMB satellites dedicated to polarization. Improving the sensitivity by a factor of 10 makes S/N from polarization comparable to the one from temperature, while the cross-correlation S/N exceeds both and would provide most of the information.

IV. CONCLUSIONS

We have analysed the prospects of measuring the projected dark matter power spectrum up to $z \sim 1100$ from the distortions induced in the CMB polarization. Any such measurement would be extremely difficult both from the temperature and polarization because of the statistical nature of such a detection. On the other hand, it would provide a direct detection of dark matter clustering on very large scales and high redshifts, possibly not attainable by any other method. For this reason it is important that any such detection from temperature fluctuations, described in [9], is independently confirmed. Such a confirmation is possible with polarization, with which one would be provided in total with 10 power spectra of convergence, all of which have to agree with each other.

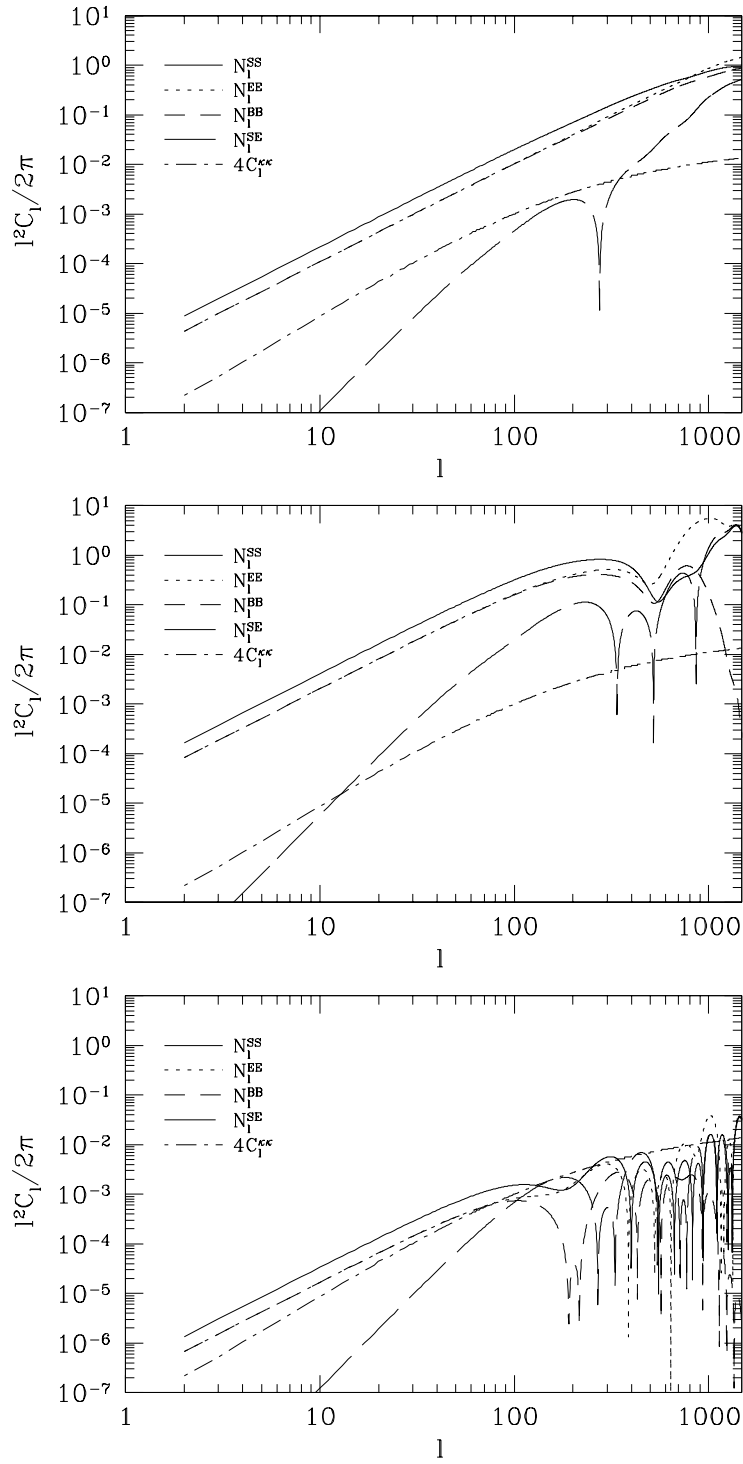


FIG. 4. Noise power spectra for temperature (upper panel), polarization (middle panel) and cross-correlation (lower panel) measurements. All contain additional noise introduced by Planck detector.

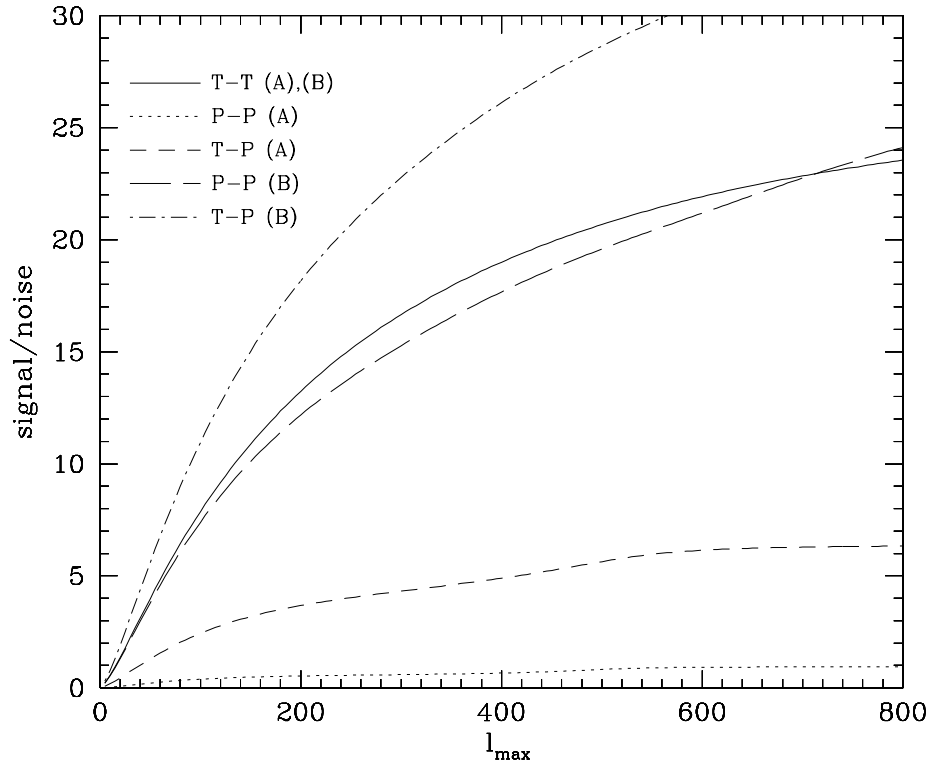


FIG. 5. Signal to noise ratio as a function of maximum multipole taken into account for temperature autocorrelation (T-T), polarization autocorrelation (P-P) and cross-correlation (T-P). The detector configurations are the same as in fig.3 . For T-T we use $w_T^{-1} = 0.002\mu K$ and $\sigma_{FWHM} = 0.12^\circ$.

Because polarization is an order of magnitude smaller than temperature fluctuations its detection will be rather limited with the planned CMB experiments including Planck. The expected signal to noise for convergence power spectrum for Planck is around unity using polarization information only, compared to 15-25 from temperature. Cross-correlation could be more promising and could provide $S/N \sim 5$ or a factor of two larger or smaller depending on the actual amount of power in convergence. The real promise of this method lies in the contemplated post-Planck experiments dedicated to polarization. Such an experiment would need to cover a significant fraction of the sky to measure the projected power spectrum on large scales. If the sensitivity of detectors is reduced by another order of magnitude over Planck then measurement of dark matter power spectrum with polarization becomes very significant and would extend the amount of information from temperature alone. It would also allow for many cross-checks of the results to reduce the possible systematics.

J.G. was supported by grant 2-P03D-022-10 from Polish State Committee for Scientific Research. U.S. acknowledges the support of NASA grant NAG5-8084. M.Z. is supported by NASA through Hubble Fellowship grant HF-01116.01-98A from STScI, operated by AURA, Inc. under NASA contract NAS5-26555. J.G. and U.S. would like to thank Max-Planck Institut für Astrophysik, Garching, for hospitality during the visits.

† Electronic address: guzik@oa.uj.edu.pl

‡ Electronic address: uros@feynman.princeton.edu

†† Electronic address: matiasz@ias.edu

- [1] Seljak U., *Astrophys. J.* **463**, 1 (1996).
- [2] Blanchard, A. and Schneider, J., *Astron. & Astrophys.* **184**, 1 (1987); Cole, S. and Efstathiou, G., *Mon. Not. Roy. Astron. Soc.* **239**, 195 (1989); Cayón, L., Martínez-González, E., & Sanz, J. L. *Astrophys. J.* **403**, 471 (1993); *ibid* *Astrophys. J.* **489**, 21 (1997).
- [3] Metcalf R. B., & Silk J. *Astrophys. J.* **492**, 1 (1998).
- [4] Benabed K., Bernardeau F., astro-ph/9906161
- [5] Zaldarriaga M. & Seljak U., *Phys.Rev. D*, **58**, 3003 (1998)
- [6] Chandrasekhar S. 1950, *Radiative Transfer*, Oxford at the Clarendon Press
- [7] Seljak U. & Zaldarriaga M., *Phys.Rev.Lett.* 82 (1999) 2636-2639
- [8] Zaldarriaga M. & Seljak U., *Phys.Rev. D*, **55**, 1830 (1997)
- [9] Zaldarriaga M. & Seljak U., *Phys.Rev. D*, astro-ph/9810257
- [10] Ostriker J. P. and Steinhardt P. J., *Nature*, **377**, 600 (1995)
- [11] Tegmark M., Taylor A.N., Heavens A.F., *Astrophys. J.* **480**, 22 (1997)
- [12] Seljak U., *Astrophys. J.* **482**, 6 (1997)
- [13] Zaldarriaga M. & Seljak U., *Phys.Rev. D*, **58**, 023003, (1998)

APPENDIX A: CORRELATION FUNCTIONS FORMULAS

Here we present correlation functions of derivatives of the CMB temperature and polarization fields. Due to the rotational invariance of the variables \mathcal{S}_T , \mathcal{S}_P , \mathcal{E}_T , \mathcal{E}_P it is enough to consider correlations between two directions separated by θ along the x direction. During derivation of the correlation functions we make use of the integral representation of Bessel functions and the CMB spectra defined in [12]. Weighted spectra $C_i(\theta)$ are defined as

$$C_i^{\tilde{A}\tilde{B}} = \int \frac{l^3 dl}{2\pi} C_l^{\tilde{A}\tilde{B}} J_i(l\theta), \quad (\text{A1})$$

where \tilde{A} and \tilde{B} stand for \tilde{T} or \tilde{P} . Some calculations yields the following correlation functions

$$C_{xx}^{QQ}(\theta) \equiv \langle \tilde{Q}_x(0) \tilde{Q}_x(\theta) \rangle_{CMB} \quad (\text{A2})$$

$$= (2\pi)^{-2} \int d^2\mathbf{l} e^{i\mathbf{l}\cdot\theta \cos\phi_l} l^2 \cos^2\phi_l C_l^{\tilde{P}\tilde{P}} \cos^2 2\phi_l$$

$$\begin{aligned}
&= \int \frac{ldl}{2\pi} l^2 C_l^{\tilde{P}\tilde{P}} \frac{1}{4} [J_0(l\theta) - 3/2J_2(l\theta) + J_4(l\theta) - 1/2J_6(l\theta)] \\
&\equiv \frac{1}{4} [C_0^{\tilde{P}\tilde{P}}(\theta) - 3/2C_2^{\tilde{P}\tilde{P}}(\theta) + C_4^{\tilde{P}\tilde{P}}(\theta) - 1/2C_6^{\tilde{P}\tilde{P}}(\theta)] \\
C_{yy}^{QQ}(\theta) &\equiv \langle \tilde{Q}_y(0)\tilde{Q}_y(\theta) \rangle_{CMB} \\
&= (2\pi)^{-2} \int d^2\mathbf{l} e^{i\mathbf{l}\cdot\theta \cos \phi_l} l^2 \sin^2 \phi_l C_l^{\tilde{P}\tilde{P}} \cos^2 2\phi_l \\
&= \int \frac{ldl}{2\pi} l^2 C_l^{\tilde{P}\tilde{P}} \frac{1}{4} [J_0(l\theta) + 3/2J_2(l\theta) + J_4(l\theta) + 1/2J_6(l\theta)] \\
&= \frac{1}{4} [C_0^{\tilde{P}\tilde{P}}(\theta) + 3/2C_2^{\tilde{P}\tilde{P}}(\theta) + C_4^{\tilde{P}\tilde{P}}(\theta) + 1/2C_6^{\tilde{P}\tilde{P}}(\theta)] \\
C_{xy}^{QQ}(\theta) &\equiv \langle \tilde{Q}_x(0)\tilde{Q}_y(\theta) \rangle_{CMB} \\
&= (2\pi)^{-2} \int d^2\mathbf{l} e^{i\mathbf{l}\cdot\theta \cos \phi_l} l^2 \sin \phi_l \cos \phi_l C_l^{\tilde{P}\tilde{P}} \cos^2 2\phi_l \\
&= 0 \\
C_{xx}^{UU}(\theta) &\equiv \langle \tilde{U}_x(0)\tilde{U}_x(\theta) \rangle_{CMB} \\
&= (2\pi)^{-2} \int d^2\mathbf{l} e^{i\mathbf{l}\cdot\theta \cos \phi_l} l^2 \cos^2 \phi_l C_l^{\tilde{P}\tilde{P}} \sin^2 2\phi_l \\
&= \int \frac{ldl}{2\pi} l^2 C_l^{\tilde{P}\tilde{P}} \frac{1}{4} [J_0(l\theta) - 1/2J_2(l\theta) - J_4(l\theta) + 1/2J_6(l\theta)] \\
&= \frac{1}{4} [C_0^{\tilde{P}\tilde{P}}(\theta) - 1/2C_2^{\tilde{P}\tilde{P}}(\theta) - C_4^{\tilde{P}\tilde{P}}(\theta) + 1/2C_6^{\tilde{P}\tilde{P}}(\theta)] \\
C_{yy}^{UU}(\theta) &\equiv \langle \tilde{U}_y(0)\tilde{U}_y(\theta) \rangle_{CMB} \\
&= (2\pi)^{-2} \int d^2\mathbf{l} e^{i\mathbf{l}\cdot\theta \cos \phi_l} l^2 \sin^2 \phi_l C_l^{\tilde{P}\tilde{P}} \sin^2 2\phi_l \\
&= \int \frac{ldl}{2\pi} l^2 C_l^{\tilde{P}\tilde{P}} \frac{1}{4} [J_0(l\theta) + 1/2J_2(l\theta) - J_4(l\theta) - 1/2J_6(l\theta)] \\
&= \frac{1}{4} [C_0^{\tilde{P}\tilde{P}}(\theta) + 1/2C_2^{\tilde{P}\tilde{P}}(\theta) - C_4^{\tilde{P}\tilde{P}}(\theta) - 1/2C_6^{\tilde{P}\tilde{P}}(\theta)] \\
C_{xy}^{UU}(\theta) &\equiv \langle \tilde{U}_x(0)\tilde{U}_y(\theta) \rangle_{CMB} \\
&= (2\pi)^{-2} \int d^2\mathbf{l} e^{i\mathbf{l}\cdot\theta \cos \phi_l} l^2 \sin \phi_l \cos \phi_l C_l^{\tilde{P}\tilde{P}} \sin^2 2\phi_l \\
&= 0 \\
C_{xx}^{TQ}(\theta) &\equiv \langle \tilde{T}_x(0)\tilde{Q}_x(\theta) \rangle_{CMB} \\
&= (2\pi)^{-2} \int d^2\mathbf{l} e^{i\mathbf{l}\cdot\theta \cos \phi_l} l^2 \cos^2 \phi_l C_l^{\tilde{T}\tilde{P}} \cos 2\phi_l \\
&= \int \frac{ldl}{2\pi} l^2 C_l^{\tilde{T}\tilde{P}} \frac{1}{4} [J_0(l\theta) - 2J_2(l\theta) + J_4(l\theta)] \\
&= \frac{1}{4} [C_0^{\tilde{T}\tilde{P}}(\theta) - 2C_2^{\tilde{T}\tilde{P}}(\theta) + C_4^{\tilde{T}\tilde{P}}(\theta)] \\
C_{yy}^{TQ}(\theta) &\equiv \langle \tilde{T}_y(0)\tilde{Q}_y(\theta) \rangle_{CMB} \\
&= (2\pi)^{-2} \int d^2\mathbf{l} e^{i\mathbf{l}\cdot\theta \cos \phi_l} l^2 \sin^2 \phi_l C_l^{\tilde{T}\tilde{P}} \cos 2\phi_l \\
&= - \int \frac{ldl}{2\pi} l^2 C_l^{\tilde{T}\tilde{P}} \frac{1}{4} [J_0(l\theta) + 2J_2(l\theta) + J_4(l\theta)] \\
&= -\frac{1}{4} [C_0^{\tilde{T}\tilde{P}}(\theta) + 2C_2^{\tilde{T}\tilde{P}}(\theta) + C_4^{\tilde{T}\tilde{P}}(\theta)] \\
C_{xy}^{TQ}(\theta) &\equiv \langle \tilde{T}_x(0)\tilde{Q}_y(\theta) \rangle_{CMB}
\end{aligned}$$

$$\begin{aligned}
&= (2\pi)^{-2} \int d^2\mathbf{l} e^{i\mathbf{l}\cdot\theta \cos \phi_l} l^2 \sin \phi_l \cos \phi_l C_l^{\tilde{T}\tilde{P}} \cos 2\phi_l \\
&= 0
\end{aligned}$$

$$\begin{aligned}
C_{xx}^{TU}(\theta) &\equiv \langle \tilde{T}_x(0) \tilde{U}_x(\theta) \rangle_{CMB} \\
&= (2\pi)^{-2} \int d^2\mathbf{l} e^{i\mathbf{l}\cdot\theta \cos \phi_l} l^2 \cos^2 \phi_l C_l^{\tilde{T}\tilde{P}} \sin 2\phi_l \\
&= 0
\end{aligned}$$

$$\begin{aligned}
C_{yy}^{TU}(\theta) &\equiv \langle \tilde{T}_y(0) \tilde{U}_y(\theta) \rangle_{CMB} \\
&= (2\pi)^{-2} \int d^2\mathbf{l} e^{i\mathbf{l}\cdot\theta \cos \phi_l} l^2 \sin^2 \phi_l C_l^{\tilde{T}\tilde{P}} \sin 2\phi_l \\
&= 0
\end{aligned}$$

$$\begin{aligned}
C_{xy}^{TU}(\theta) &\equiv \langle \tilde{T}_x(0) \tilde{U}_y(\theta) \rangle_{CMB} \\
&= (2\pi)^{-2} \int d^2\mathbf{l} e^{i\mathbf{l}\cdot\theta \cos \phi_l} l^2 \sin \phi_l \cos \phi_l C_l^{\tilde{T}\tilde{P}} \sin 2\phi_l \\
&= \int \frac{l dl}{2\pi} l^2 C_l^{\tilde{T}\tilde{P}} \frac{1}{4} [J_0(l\theta) - J_4(l\theta)] \\
&= \frac{1}{4} [C_0^{\tilde{T}\tilde{P}}(\theta) - C_4^{\tilde{T}\tilde{P}}(\theta)]
\end{aligned}$$

$$\begin{aligned}
C_{xx}^{QU}(\theta) &\equiv \langle \tilde{Q}_x(0) \tilde{U}_x(\theta) \rangle_{CMB} \\
&= (2\pi)^{-2} \int d^2\mathbf{l} e^{i\mathbf{l}\cdot\theta \cos \phi_l} l^2 \cos^2 \phi_l C_l^{\tilde{P}\tilde{P}} \sin 2\phi_l \cos 2\phi_l \\
&= 0
\end{aligned}$$

$$\begin{aligned}
C_{yy}^{QU}(\theta) &\equiv \langle \tilde{Q}_y(0) \tilde{U}_y(\theta) \rangle_{CMB} \\
&= (2\pi)^{-2} \int d^2\mathbf{l} e^{i\mathbf{l}\cdot\theta \cos \phi_l} l^2 \sin^2 \phi_l C_l^{\tilde{P}\tilde{P}} \sin 2\phi_l \cos 2\phi_l \\
&= 0
\end{aligned}$$

$$\begin{aligned}
C_{xy}^{QU}(\theta) &\equiv \langle \tilde{Q}_x(0) \tilde{U}_y(\theta) \rangle_{CMB} \\
&= (2\pi)^{-2} \int d^2\mathbf{l} e^{i\mathbf{l}\cdot\theta \cos \phi_l} l^2 \sin \phi_l \cos \phi_l C_l^{\tilde{P}\tilde{P}} \sin 2\phi_l \cos 2\phi_l \\
&= - \int \frac{l dl}{2\pi} l^2 C_l^{\tilde{P}\tilde{P}} \frac{1}{8} [J_2(l\theta) - J_6(l\theta)] \\
&= -\frac{1}{8} [C_2^{\tilde{P}\tilde{P}}(\theta) - C_6^{\tilde{P}\tilde{P}}(\theta)].
\end{aligned}$$